The Astrophysical Journal, 700:L16–L20, 2009 July 20 doi:10.1088/0004-637X/700/1/L16

A MAGNETIC RECONNECTION MECHANISM FOR ION ACCELERATION AND ABUNDANCE ENHANCEMENTS IN IMPULSIVE FLARES

J. F. Drake[1], P. A. Cassak[2], M. A. Shay[3], M. Swisdak[1], and E. Quataert[4]
[1] University of Maryland, College Park, MD 20742, USA; drake@umd.edu, swisdak@umd.edu
[2] West Virginia University, Morgantown, WV 26506, USA; paul.cassak@mail.wvu.edu
[3] University of Delaware, Newark, DE 19716, USA; shay@physics.udel.edu
[4] University of California, Berkeley, CA 94720, USA; eliot@astro.berkeley.edu
Received 2009 April 22; accepted 2009 June 12; published 2009 June 29

ABSTRACT

The acceleration of ions during magnetic reconnection in solar flares is explored with simulations and analytic analysis. Ions crossing into Alfvénic reconnection outflows can behave like pickup particles and gain an effective thermal velocity equal to the Alfvén speed. However, with a sufficiently strong ambient out-of-plane magnetic field, which is the relevant configuration for flares, the ions can become adiabatic and their heating is then dramatically reduced. The threshold for nonadiabatic behavior, where ions are strongly heated, becomes a condition on the ion mass-to-charge ratio, $m_i/m_pZ_i > 10\sqrt{\beta_{0x}/2}/\pi$, where m_i and Z_i are the ion mass and charge state, m_p is the proton mass, and $\beta_{0x} = 8\pi nT/B_{0x}^2$ is the ratio of the plasma pressure to that of the reconnecting magnetic field B_{0x}. Thus, during flares high mass-to-charge particles gain energy more easily than protons and a simple model reveals that their abundances are enhanced, which is consistent with observations.

Key words: acceleration of particles – solar wind – Sun: corona – Sun: flares

1. INTRODUCTION

In solar flares, magnetic reconnection converts stored magnetic energy in the corona into high-velocity flows and energetic particles. A significant fraction of this released energy is transferred to energetic electrons and ions, with ions reaching energies in the range of GeV (Lin et al. 2003; Emslie et al. 2004). The acceleration mechanism for these energetic ions remains unknown although models based on particle interaction with multiple magnetic islands in two dimension (Matthaeus et al. 1984; Kliem 1994; Shibata & Tanuma 2001) and three dimension (Onofri et al. 2006) and with magnetohydrodynamic waves (Miller 1998; Petrosian & Liu 2004) have been proposed.

Further information on the particle acceleration mechanism in impulsive flares has been deduced from measurements of the energy spectra of trace elements: the abundance of high mass-to-charge (M/Q) ions is greatly enhanced compared with coronal values (Reames et al. 1994; Mason et al. 1994; Reames & Ng 2004). The energy spectra of the various species display a common shape (Mason et al. 1994) and the size of the enhancement factor depends only on M/Q (Mason 2007). Magnetohydrodynamic wave models provide an intuitive explanation for these observations (Miller 1998; Liu et al. 2006): high M/Q ions resonate with and gain energy from lower-frequency/longer-wavelength waves, which are expected to have larger amplitudes. On the other hand, the extraordinary efficiency of particle acceleration in flares (Lin & Hudson 1971; Emslie et al. 2004) requires that the wave generation mechanism in flares must also be very efficient—at present no mechanism with the required efficiency has been identified. If abundance enhancements in impulsive flares could be directly attributed to magnetic reconnection, the need for invoking wave mechanisms and their associated efficiency requirements could be sidestepped.

In an earlier paper (Drake et al. 2009), we showed that in the case of magnetic reconnection with antiparallel magnetic fields that ions entering the Alfvénic outflow from the x-line behave like pickup particles (Mobius et al. 1985)—that is, they cross a narrow boundary layer and find themselves nearly at rest in a high-velocity magnetized plasma. As a result, they gain a convective velocity equal to the reconnection exhaust velocity and an equal thermal velocity. Since reconnection with an ambient out-of-plane (guide) magnetic field is the more generic case in flares, an important question is whether the same pickup mechanism is responsible for ion heating when the guide field becomes equal to or larger than the reconnecting field. Specifically, in flares can the guide field effectively magnetize small M/Q ions so that their motion is adiabatic and their heating reduced compared with high M/Q ions? Could such a mechanism explain the observations of abundance enhancements in impulsive flares?

In this Letter, we explore ion heating and acceleration during magnetic reconnection with an ambient guide field. We first carry out PIC simulations that demonstrate that the ion temperature increases sharply across a narrow boundary layer that separates the upstream plasma from the Alfvénic exhaust. As a result, the ion heating during reconnection is dominated by the large-scale outflow exhausts rather than the x-line proper. During reconnection with a large guide field, however, ion heating decreases dramatically compared with that during antiparallel reconnection. By following the dynamics of test particles, we show that this reduction is a consequence of the transition of the ions to adiabatic behavior as they cross the narrow layer bounding the plasma outflow. This boundary layer has a characteristic scale length equal to ρ_s, the ion Larmor radius based on the sound speed. We show that only ions above a critical mass-to-charge ratio, M/Q, are nonadiabatic. The trajectories reveal that these ions become demagnetized as they cross the exhaust boundary. Upon entering the exhaust, they are essentially at zero velocity within a local plasma flowing at the Alfvén speed. As a result, they behave like classic pickup particles (Mobius et al. 1985) and gain an effective thermal speed equal to the exhaust velocity once they have been "picked up" by the exhaust. Ions with M/Q below this threshold are adiabatic and simply convect with the outflow with very little heating. These results provide an alternative to the wave model

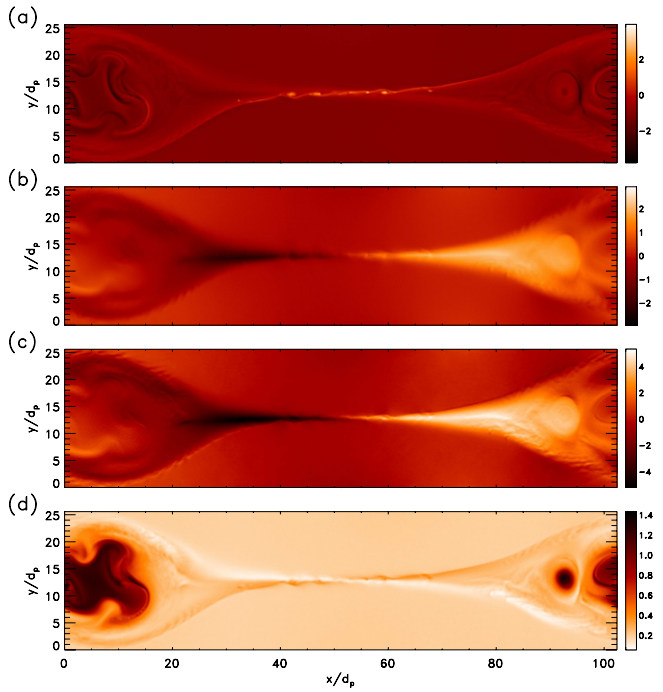

Figure 1. Shown are plots of (a) the electron out-of-plane current J_{ez}, (b) the ion outflow velocity v_{px}, (c) the electric field E_y, and (d) the electron density n from a PIC simulation with an initial guide field $B_{0z} = 2.0B_{0x}$.

for understanding abundance enhancements of high M/Q ions in impulsive flares (Mason 2007).

2. NUMERICAL SIMULATIONS

Our simulations are performed with the PIC code p3d (Zeiler et al. 2002) and the Hall MHD code f3d (Shay et al. 2004). The results are presented in normalized units: the magnetic field to the asymptotic value of the reversed field B_{0x}, the density to the value at the center of the current sheet minus the uniform background density, velocities to the proton Alfvén speed $c_{\rm Apx} = B_{0x}/\sqrt{4\pi m_p n_0}$, times to the inverse proton cyclotron frequency in B_{0x}, $\Omega_{\rm px}^{-1} = m_p c/eB_{0x}$, lengths to the proton inertial length $d_p = c_{\rm Apx}/\Omega_{\rm px}$, and temperatures to $m_p c_{\rm Apx}^2$. The normalization of f3d differs slightly from that of p3d in that the density is normalized to the asymptotic value. We consider a system periodic in the x–y plane where flow into and away from the x-line are parallel to $\hat{\mathbf{y}}$ and $\hat{\mathbf{x}}$, respectively. The reconnection electric field is parallel to $\hat{\mathbf{z}}$. The initial equilibrium consists of two Harris current sheets superimposed on an ambient background population of uniform density. The reconnection magnetic field is given by $B_x = \tanh[(y-L_y/4)/w_0] - \tanh[(y-3L_y/4)/w_0] - 1$, where w_0 and L_y are the half-width of the initial current sheets and the box size in the $\hat{\mathbf{y}}$ direction. Since we are focusing on the ion dynamics, which requires as large a simulation domain as possible, we minimize the separation of scales by using an ion to electron mass ratio of 25. The rate of magnetic reconnection and structure of the outflow exhaust are insensitive to this ratio (Shay & Drake 1998; Hesse et al. 1999; Shay et al. 2007; Drake et al. 2008). Ion heating, which depends on the exhaust geometry, is therefore also not sensitive to the mass ratio. The initial density profile is the Harris form plus a uniform background of 0.2 for p3d and 1.0 for f3d. The simulations are two dimensional and reconnection is initiated with a small initial magnetic perturbation that produces a single magnetic island on each current layer.

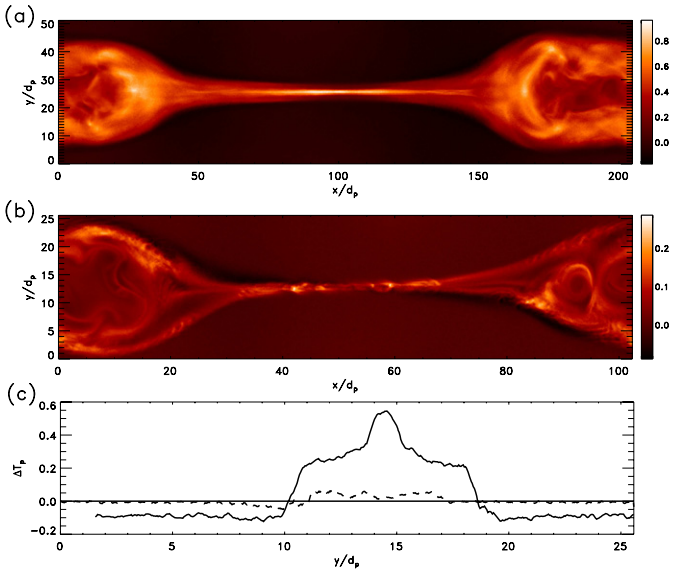

Figure 2. The ion temperature from two PIC simulations, one with $B_{0z} = 0$ in (a) and one with $B_{0z} = 2.0B_{0x}$ in (b). Note the different ranges of color scales for the two plots. Cuts of the ion temperature change ΔT_p across the exhaust for $B_{0z} = 0$ (solid) and $B_{0z} = 2.0B_{0x}$ (dashed).

In Figure 1, we show the results of a p3d simulation with an initial guide field B_{0z} of $2.0B_{0x}$ in a computational domain $L_x \times L_y = 102.4d_p \times 51.2d_p$ at $t = 96.0\Omega_{px}^{-1}$. The grid spacing for this run is $0.025d_p$, the electron and proton temperatures, $T_e = T_p = 0.25m_p c_{\rm Apx}^2$, are initially uniform and the velocity of light is $20c_{\rm Apx}$. In Figure 1(a) is the electron out-of-plane current J_{ez} centered around the x-line. Secondary islands are a typical feature of reconnection with a guide field (Drake et al. 2006b) but at this time the secondary islands have convected downstream. In Figure 1(b) is the ion outflow v_{px} from the x-line and in Figure 1(c) is the corresponding electric field E_y, which drives the outflow during reconnection with a guide field, $v_{px} \sim cE_y/B_z$. The strong correlation between v_{px} and E_y is evident. Finally, in Figure 1(d) we show the ion density. Evident are the low-density cavities, on two of the four separatrices (Pritchett & Coroniti 2004; Drake et al. 2005), which are evidence for the role of the kinetic Alfvén wave in driving the outflow from the x-line. We will later show data demonstrating that the characteristic scale length of the kinetic Alfvén wave in the direction perpendicular to the magnetic field, $\rho_{\rm sp} = c_{\rm sp}/\Omega_{\rm pz}$ with $c_{\rm sp} = \sqrt{(T_e + T_p)/m_p}$ the proton sound speed, controls the thickness of the boundary layer separating the upstream plasma from the exhaust. The scale length of the rise in E_y across this boundary in particular controls whether the ions crossing into the exhaust behave adiabatically or not.

In Figure 2, we compare the ion temperature increments, $\Delta T_p = T_p - T_{p0}$, from two simulations, one with $B_{0z} = 0$ (Shay et al. 2007) in Figure 2(a) and the second in Figure 2(b) corresponding to the run of Figure 1. In both cases, the ion temperature jumps sharply within the exhaust. However, note that the scales on the two plots differ, the jump in ion temperature in the case of $B_{0z} = 0$ being more that three times that of the case $B_{0z} = 2.0B_{0x}$. This can be seen more clearly in Figure 2(c), where we show cuts of the ion temperature across the exhaust at $x = 128d_p$ (solid) for $B_{0z} = 0$ at $x = 81.0d_p$ (dashed) for $B_{0z} = 2.0B_{0x}$. The location of the cut in the antiparallel case was chosen at a location where the width of the exhaust approximately matched that of $B_{0z} = 2.0$. We emphasize that

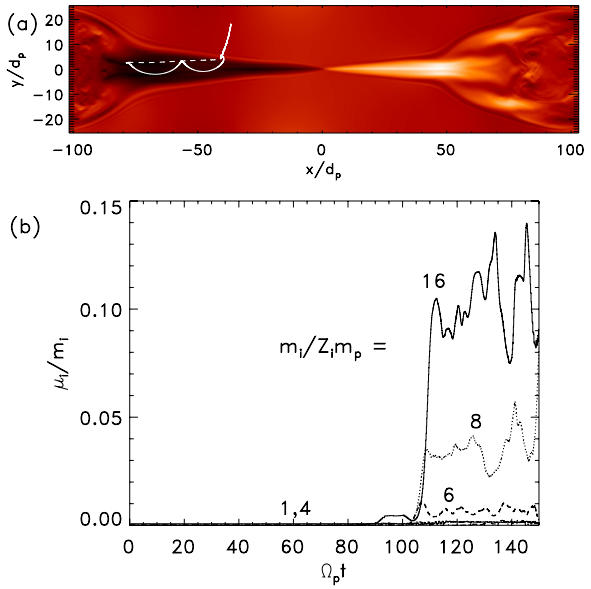

Figure 3. (a) Test particle trajectories of a proton (dashed) and an ion with a mass of $16m_p$ (solid) calculated from the fields of a Hall MHD reconnection simulation with $B_{0z} = 5.0B_{0x}$. The background is the electric field E_y. (b) The magnetic moment $\mu_i = m_i\delta v_\perp^2/2B$ vs. time of test ions of various masses. Protons and alpha particles are adiabatic, while higher mass particles exhibit a jump in μ_i as they cross the exhaust boundary.

the lower ion heating for $B_{0z} = 2.0B_{0x}$ is not because of a smaller rate of reconnection, which at $0.15c_{\rm Apx}B_{0x}/c$ was close to that of the antiparallel simulation (Shay et al. 2007).

3. ORBITS AND ION PICKUP

The temperature increase of ions within the outflow exhaust in the case of antiparallel reconnection was attributed to the "pickup" behavior of ions as they crossed the narrow layer bounding the outflow from the x-line (Drake et al. 2009). Upon crossing the boundary layer, the ions are suddenly in a high-velocity streaming plasma and are picked up by this flowing plasma in a manner that is similar to the pickup of a newly ionized particle in the solar wind (Mobius et al. 1985). To understand why this mechanism is less efficient in the case of a guide field, we have studied test particle trajectories of ions of various masses in the fields from reconnection simulations. We show in Figure 3(a) the orbits of a proton and a particle with a mass $m_i = 16m_p$ over a background of E_y. The data is from a Hall MHD simulation with a guide field of $5.0B_{0x}$ in a $L_x \times L_y = 204.8d_p \times 102.4d_p$ computational domain (Cassak et al. 2007). This simulation has a much larger guide field than could be used in a comparably sized PIC simulation. The proton, shown by the dashed line, enters the exhaust and immediately moves downstream in the direction of the local $\mathbf{E} \times \mathbf{B}$ drift. In Figure 3(b), in which the time evolution of the magnetic moments $\mu_i = m_i\delta v_\perp^2/2B$ of ions of various mass are shown, where $\delta v_\perp$ is the ion perpendicular velocity with the $\mathbf{E}\times\mathbf{B}$ drift subtracted. The proton exhibits essentially no jump in magnetic moment on entry into the exhaust. In contrast, the mass $16m_p$ particle exhibits the cusp-like trajectory of classic pickup particles (solid line in Figure 3(a)) and its magnetic moment jumps sharply as it crosses the exhaust boundary (Figure 3(b)). Thus, the mass $16m_p$ behaves like a pickup particle while the proton does not.

The transition between adiabatic and pickup-like behavior depends on the transit time across the boundary layer as the ions enter the exhaust compared with their cyclotron period. For a boundary layer of thickness Δ, the effective wavevector is π/Δ and the condition for nonadiabatic behavior becomes $\pi v_{\rm in}/\Delta > \Omega_{iz}$, where $v_{\rm in}$ is the inflow velocity into the exhaust (the reconnection inflow velocity) and Ω_{iz} is the cyclotron frequency in the guide field. The kinetic Alfvén wave controls the exhaust boundary in the limit of a large guide field and the scale length ρ_s is the expected scale length (Coroniti 1971; Kleva et al. 1995; Cassak et al. 2007). To test this scaling, we overlay in Figure 4 cuts across the outflow of $cE_y/B_{0z}c_{\rm Apx}$ from the PIC simulation of Figure 1 (guide field of $2.0B_{0x}$ and $x = 81.0d_p$) and from a simulation with a guide field of $1.0B_{0x}$. The latter was run on a $L_x \times L_y = 204.8d_p \times 102.4d_p$ domain with a grid spacing of $0.05d_p$ and other parameters as in the $B_{0z} = 2.0$ simulation. When the plots are overlaid on a spatial scale normalized to ρ_s, the steep portions of the boundary layer match extremely well. In units of the proton inertial scale d_p the values of ρ_s differ by a factor of two so similar plots based on the normalization to d_p do not overlay. Note that in both simulations the boundary layers on the left side of the exhaust are distinctly broader than those on the right. The density cavities that map the separatrices on the left boundaries of the exhausts disrupt the boundary layers (see Figure 1(d)). Taking the boundary layer thickness to be ρ_s and the inflow velocity $v_{\rm in} = 0.1c_{\rm Apx}$, we obtain the threshold for pickup behavior in the strong guide-field limit,

$$\frac{m_i}{m_p Z_i} > \frac{10}{\pi}\frac{c_{\rm sp}}{c_{\rm Apx}} = \frac{10}{\pi\sqrt{2}}\sqrt{\beta_{\rm px}}, \qquad (1)$$

where $\beta_{\rm px} = 8\pi n(T_e+T_p)/B_{0x}^2$ is based on the reconnecting field B_{0x}. This threshold is independent of the guide field because the guide field dependence of the gyrofrequency and boundary layer thickness cancel. For the simulation of Figure 3, in which $\beta_{\rm px} = 5.0$, the threshold condition is $m_i/Z_im_p > 5.0$, which is close to the threshold for nonadiabatic behavior seen in the time dependence of μ in Figure 3(b). For the PIC simulation of Figure 1 with $B_{0z} = 2.0B_{0x}$, $\beta_{\rm px} = 0.2$ and the threshold is $m_i/Z_im_p > 1.4$, so protons should remain nearly adiabatic, which is consistent with the weak heating in this simulation.

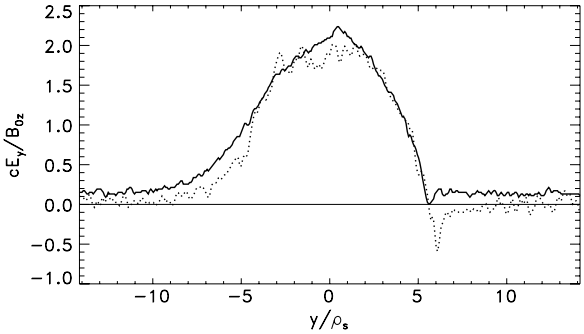

Figure 4. Plots of E_y across the exhaust from PIC simulations with $B_{0z} = 2.0B_{0x}$ (solid) and $B_{0z} = 1.0B_{0x}$ (dotted). The y coordinate is normalized to the ion sound Larmor radius $\rho_{\rm sp} = c_{\rm sp}/\Omega_{\rm pz}$.

4. ION HEATING

To better understand how ions gain energy on entry into the exhaust, we examine the structure of the electric and magnetic fields within and just upstream of the exhaust. Cuts from the Hall MHD simulation of Figure 3 are shown in Figure 5 at $x = -47.1d_p$, which is near the exhaust entry point of the trajectories shown in Figure 3. The magnetic field B_y is nearly constant

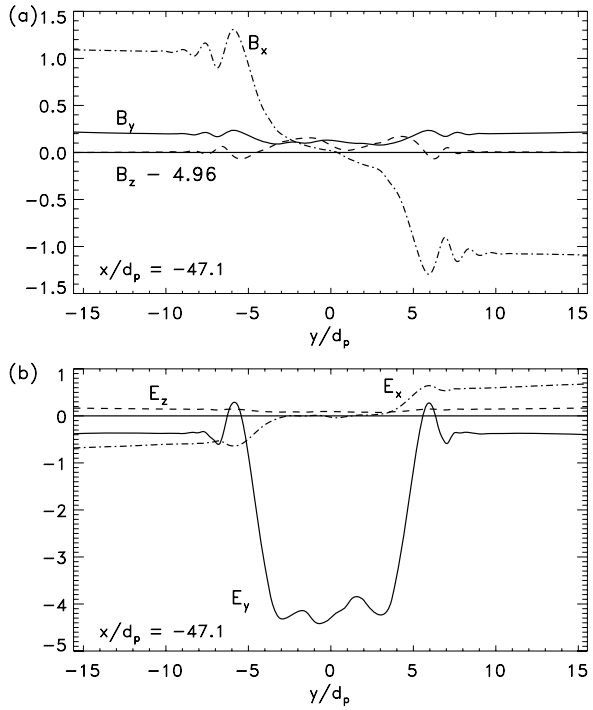

Figure 5. Cuts across the exhaust at $x = -47.1d_i$ of the components of the magnetic field in (a) and the electric field in (b) from the Hall MHD simulation of Figure 3.

across the exhaust, while B_x decreases sharply at the boundary, which is consistent with the switch-off behavior of Petschek slow shocks (Petschek 1964; Coroniti 1971). Cuts through the outflow of the PIC simulation of Figure 1 are similar. Within the exhaust the dominant electric field is $E_y \sim -E_z B_{0z}/B_y$, which develops to force $\mathbf{E}\cdot\mathbf{B} = 0$. E_x is small in the exhaust but rises sharply upstream of the exhaust such that $E_x \sim -E_z B_{0z}/B_{0x}$ so that outside of the exhaust again $\mathbf{E}\cdot\mathbf{B} = 0$. Thus,

$$\mathbf{E}_{\rm up} = \left(-\frac{E_z B_{0z}}{B_{0x}}, 0, E_z\right); \qquad \mathbf{E}_{\rm exh} = \left(0, -\frac{E_z B_{0z}}{B_y}, E_z\right). \tag{2}$$

Transforming to the moving frame $v_x \equiv -v_0 = -cE_z/B_y$, the fields $\mathbf{E}'$ become

$$\mathbf{E}'_{\rm up} = \left(-\frac{E_z B_{0z}}{B_{0x}}, \frac{E_z B_{0z}}{B_y}, 0\right); \qquad \mathbf{E}'_{\rm exh} = 0. \tag{3}$$

In the upstream region in the moving frame, the ions drift with the $\mathbf{E}\times\mathbf{B}$ velocity but also have a parallel velocity

$$v_\parallel = v_0 B_{0x}/B_0, \tag{4}$$

where $B_0^2 = B_{0x}^2 + B_{0z}^2$. Particles which are adiabatic maintain their parallel streaming velocity on entry into the exhaust but do not gain a perpendicular thermal speed since μ is preserved. Once the particles entering from the two sides of the exhaust mix, the parallel streaming velocity becomes an effective thermal speed. The temperature increments are therefore

$$\Delta T_\parallel = m_i v_0^2 B_{0x}^2/B_0^2; \qquad \Delta T_\perp = 0. \tag{5}$$

The pickup ions, which satisfy the condition in Equation (1), enter the exhaust with their upstream velocity, which to lowest order in B_y is simply the exhaust velocity v_0. Since we are taking $B_x = 0$ within the exhaust, this is perpendicular to the local magnetic field and the particles simply orbit in the x–y plane around the guide field B_z, which is consistent with the orbit of the mass $16m_p$ particle in Figure 3(a). The ions eventually form a ring distribution with velocity v_0. There is no increase in the parallel temperature. The temperature increments of ions in the pickup regime are therefore

$$\Delta T_\parallel = 0; \qquad \Delta T_\perp = \tfrac{1}{2} m_i v_0^2. \tag{6}$$

In the limit of a strong guide field, the temperature increment of the pickup ions exceeds that of the adiabatic ions by the factor $B_{0z}^2/B_{0x}^2 \gg 1$.

5. DISCUSSION AND IMPLICATIONS

During magnetic reconnection with a guide field, we have shown that ions above a critical mass-to-charge ratio M/Q (see Equation (1)) behave like pickup particles as they enter the exhaust and gain significant energy, while below this threshold there is little ion heating. Reconnection in the solar corona typically takes place with a strong guide field and there is now strong evidence that during impulsive flares the abundances of high mass-to-charge ratio energetic ions are strongly enhanced and the enhancement depends only on M/Q (Mason 2007). An important question is whether the abundance enhancement of these ions is linked to the heating threshold explored in this Letter.

For a given M/Q, the threshold for heating in Equation (1) can be translated into a threshold on the reconnection magnetic field B_{0x}. For typical coronal parameters ($n \sim 10^9$ cm^{-3}, $T \sim 3\times 10^6$ K), the threshold in B_{0x} is around 10 G. MHD simulations (Shibata & Tanuma 2001) and kinetic simulations with guide fields (Drake et al. 2006a, 2006b) indicate that reconnection develops not as a single x-line but as a bath of magnetic islands. Observations of tadpole-like structures in postflare loops (McKenzie & Hudson 1999; Sheeley et al. 2004) also support such a hypothesis. During reconnection in large-scale current layers, the strength of the reconnecting field just upstream of the dissipation region B_{0x} typically increases with time as stronger fields convect toward the x-line (Cassak et al. 2006). Thus, in a multi-island picture of reconnection, larger islands correspond to larger values of B_{0x} and the threshold for ion heating can therefore be re-stated as a threshold in island size $w_{\rm th}$,

$$c_{\rm Ax} > 3.2 c_{\rm sp}\frac{m_p Z_i}{m_i} \equiv c'_{\rm Apx} w_{\rm th}, \tag{7}$$

where $c'_{\rm Ax} = (dB_{0x}/dy)/\sqrt{4\pi m_p n}$. Thus, higher mass ions have lower island width thresholds for heating. The rate of production of energetic ions during reconnection can be estimated as

$$\frac{dN_i}{dt} \propto \sum_{w>w_{\rm th}} 0.1 c_{\rm Apx} L_w \propto \sum_{w>w_{\rm th}} w^2 \propto \int_{w_{\rm th}}^{\infty} dw w^2 P(w), \tag{8}$$

where $L_w \propto w$ is the length of an island of width w and $P(w)$ is the size distribution of islands. Since $P(w)$ is unknown, we make the reasonable assumption that the distribution can be expressed as a power law, $P \propto w^{-\alpha}$. The integral over island size then yields the rate of production of energetic ions as

$$\frac{dN_i}{dt} \propto w_{\rm th}^{3-\alpha} \propto \left(\frac{m_i}{Z_i m_p}\right)^{\alpha-3}. \tag{9}$$

The rate in Equation (9) is the rate at which cold ions enter the exhausts of a bath of magnetic islands. From Equation (6),

the energy gain on a single exhaust entry for typical solar parameters ($B_{0x} \sim 100$ G, $n \sim 10^9$ cm^{-3}) is around 0.1 MeV nucleon^{-1}. Ions will need to be further accelerated to the range of 10–100 MeV nucleon^{-1} or even higher to explain the observations in intense flares. Since ions are Alfvénic after a single interaction with a reconnection exhaust, they can also undergo Fermi reflection in contracting islands as has been discussed in the context of electron acceleration (Drake et al. 2006a). We suggest that ion pickup in reconnection exhausts is the critical mechanism for seeding energetic ions and therefore controls the number of accelerated ions and therefore the enhancement factor seen in the observations. The observations suggest that the enhancement factor scales like $(m_i/Z_i m_p)^{3.26}$ (Mason 2007). The rate given in Equation (9) is consistent with the observations if $\alpha \sim 6.26$, which corresponds to a strong peaking of island probability at small island widths. The probability distribution of magnetic islands in large-scale current layers is presently being explored (R. Fermo et al. 2009, in preparation).

Reconnection associated with Alfvénic turbulence has been proposed as an ion heating mechanism in the solar wind and corona (Dmitruk et al. 2004). The threshold for ion heating given in Equation (1) suggests that because the β of the solar wind is substantial, proton heating in solar wind turbulence due to reconnection is unlikely except in regions where the reconnecting field B_{0x} is comparable to or larger than the ambient guide field. Large numbers of solar wind reconnection events with significant guide fields have recently been identified in the *Wind* spacecraft data set (Gosling 2007). This data set can potentially be used to explore whether proton heating is suppressed compared with that of alpha particles during reconnection with a strong guide field. In the corona where β is much lower, the threshold in Equation (1) is easier to satisfy.

There is also evidence for strong heating of carbon during reconnection events in reversed-field-pinch experiments (Gangadhara et al. 2007). Not all reconnection events in these experiments produce strong heating. Since these experiments are in the strong guide-field limit, the threshold condition given in Equation (1) might be the factor that determines which reconnection events produce strong ion heating.

This work has been supported by NSF grant PHY-0316197, NASA grant NNG06GH23G, and DOE grant ER54197. Computations were carried out at the National Energy Research Scientific Computing Center.

REFERENCES

Cassak, P., Drake, J. F., & Shay, M. A. 2006, ApJ, 644, L145
Cassak, P., Drake, J. F., & Shay, M. A. 2007, Phys. Plasmas, 14, 054502
Coroniti, F. V. 1971, Nucl. Fusion, 11, 261
Dmitruk, P., Matthaeus, W. H., & Seenu, N. 2004, ApJ, 617, 667
Drake, J. F., Shay, M. A., & Swisdak, M. 2008, Phys. Plasmas, 15, 042306
Drake, J. F., Shay, M. A., Thongthai, W., & Swisdak, M. 2005, Phys. Rev. Lett., 94, 095001
Drake, J. F., Swisdak, M., Che, H., & Shay, M. A. 2006a, Nature, 443, 553
Drake, J. F., Swisdak, M., Schoeffler, K. M., Rogers, B. N., & Kobayashi, S. 2006b, Geophys. Res. Lett., 33, L13105
Drake, J. F., et al. 2009, J. Geophys. Res., 114, A05111
Emslie, A. G., et al. 2004, J. Geophys. Res., 109, A10104
Gangadhara, S., Craig, D., Ennis, D. A., Hartog, D. J. D., Fiksel, G., & Prager, S. C. 2007, Phys. Rev. Lett., 98, 075001
Gosling, J. T. 2007, ApJ, 671, L73
Hesse, M., Schindler, K., Birn, J., & Kuznetsova, M. 1999, Phys. Plasmas, 5, 1781
Kleva, R., Drake, J., & Waelbroeck, F. 1995, Phys. Plasmas, 2, 23
Kliem, B. 1994, ApJ, 90, 719
Lin, R. P., & Hudson, H. S. 1971, Sol. Phys., 17, 412
Lin, R. P., et al. 2003, ApJ, 595, L69
Liu, S., Petrosian, V., & Mason, G. M. 2006, ApJ, 636, 462
Mason, G. M. 2007, Space Sci. Rev., 130, 231
Mason, G. M., Mazur, J. E., & Hamilton, D. C. 1994, ApJ, 425, 843
Matthaeus, W. H., Ambrosiano, J. J., & Goldstein, M. J. 1984, Phys. Rev. Lett., 53, 1449
McKenzie, D. E., & Hudson, H. S. 1999, ApJ, 519, 93
Miller, J. A. 1998, Space Sci. Rev., 86, 79
Mobius, E., Hovestadt, D., Klecker, B., Scholer, M., Gloeckler, G., & Ipavich, F. M. 1985, Nature, 318, 426
Onofri, M., Isliker, H., & Vlahos, L. 2006, Phys. Rev. Lett., 96, 151102
Petrosian, V., & Liu, S. 2004, ApJ, 610, 550
Petschek, H. E. 1964, in AAS/NASA Symp. on the Physics of Solar Flares, ed. W. N. Ness (Washington, DC: NASA), 425
Pritchett, P. L., & Coroniti, F. V. 2004, J. Geophys. Res., 109, A01220
Reames, D. V., Meyer, J.-P., & von Rosenvinge, T. T. 1994, ApJS, 90, 649
Reames, D. V., & Ng, C. K. 2004, ApJ, 610, 510
Shay, M. A., & Drake, J. F. 1998, Geophys. Res. Lett., 25, 3759
Shay, M. A., Drake, J. F., & Swisdak, M. 2007, Phys. Rev. Lett., 99, 155002
Shay, M. A., Drake, J. F., Swisdak, M., & Rogers, B. N. 2004, Phys. Plasmas, 11, 2199
Sheeley, N. R., Warren, H. P., & Wang, Y.-M. 2004, ApJ, 616, 1224
Shibata, K., & Tanuma, S. 2001, Earth Planets Space, 53, 473
Zeiler, A., Biskamp, D., Drake, J. F., Rogers, B. N., Shay, M. A., & Scholer, M. 2002, J. Geophys. Res., 107, 1230